RESEARCH ARTICLE OPEN ACCESS

Central Vein Sign, Cortical Lesions, and Paramagnetic Rim Lesions for the Diagnostic and Prognostic Workup of Multiple Sclerosis

Serena Borrelli, MD, Maria Sofia Martire, MD, Anna Stölting, MSc, Colin Vanden Bulcke, MSc, Edoardo Pedrini, PhD, François Guisset, MD, Céline Bugli, PhD, Halil Yildiz, MD, Lucie Pothen, MD, PhD, Sophie Elands, MD, Vittorio Martinelli, MD, Bryan Smith, MD, Steven Jacobson, PhD, Renaud A. Du Pasquier, MD, Vincent Van Pesch, MD, PhD, Massimo Filippi, MD, Daniel S. Reich, MD, PhD, Martina Absinta, MD, PhD, and Pietro Maggi, MD, PhD

Correspondence
Dr. Maggi
pietro.maggi@uclouvain.be

Neurol Neuroimmunol Neuroinflamm 2024;11:e200253. doi:10.1212/NXI.0000000000200253

Abstract

Background and Objectives

The diagnosis of multiple sclerosis (MS) can be challenging in clinical practice because MS presentation can be atypical and mimicked by other diseases. We evaluated the diagnostic performance, alone or in combination, of the central vein sign (CVS), paramagnetic rim lesion (PRL), and cortical lesion (CL), as well as their association with clinical outcomes.

Methods

In this multicenter observational study, we first conducted a cross-sectional analysis of the CVS (proportion of CVS-positive lesions or simplified determination of CVS in 3/6 lesions—Select3*/Select6*), PRL, and CL in MS and non-MS cases on 3T-MRI brain images, including 3D T2-FLAIR, T2*-echo-planar imaging magnitude and phase, double inversion recovery, and magnetization prepared rapid gradient echo image sequences. Then, we longitudinally analyzed the progression independent of relapse and MRI activity (PIRA) in MS cases over the 2 years after study entry. Receiver operating characteristic curves were used to test diagnostic performance and regression models to predict diagnosis and clinical outcomes.

Results

The presence of ≥41% CVS-positive lesions/≥1 CL/≥1 PRL (optimal cutoffs) had 96%/90%/93% specificity, 97%/84%/60% sensitivity, and 0.99/0.90/0.77 area under the curve (AUC), respectively, to distinguish MS (n = 185) from non-MS (n = 100) cases. The Select3*/Select6* algorithms showed 93%/95% specificity, 97%/89% sensitivity, and 0.95/0.92 AUC. The combination of CVS, CL, and PRL improved the diagnostic performance, especially when Select3*/Select6* were used (93%/94% specificity, 98%/96% sensitivity, 0.99/0.98 AUC; p = 0.002/p < 0.001). In MS cases (n = 185), both CL and PRL were associated with higher MS disability and severity. Longitudinal analysis (n = 61) showed that MS cases with >4 PRL at baseline were more likely to experience PIRA at 2-year follow-up (odds ratio 17.0, 95% confidence interval: 2.1–138.5; p = 0.008), whereas no association was observed between other baseline MRI measures and PIRA, including the number of CL.

From the Neuroinflammation Imaging Lab (NIL) (S.B., A.S., C.V.B., F.G., P.M.), Institute of NeuroScience, Université catholique de Louvain; Department of Neurology (S.B., S.E.), Hôpital Erasme, Hôpital Universitaire de Bruxelles; Department of Neurology (S.B.), Centre Hospitalier Universitaire Brugmann, Université Libre de Brussels, Belgium; Neurology Unit (M.S.M., V.M., M.F.), IRCCS San Raffaele Hospital, Milan, Italy; ICTEAM Institute (C.V.B.), Université catholique de Louvain, Louvain-la-Neuve, Belgium; Vita-Salute San Raffaele University (E.P., M.F., M.A.); Translational Neuropathology Unit (E.P., M.A.), Division of Neuroscience, IRCCS San Raffaele Scientific Institute, Milan, Italy; Plateforme technologique de Support en Méthodologie et Calcul Statistique (C.B.); Department of Internal Medicine and Infectious Diseases (H.Y., L.P.), Cliniques Universitaires Saint-Luc, Université catholique de Louvain, Brussels, Belgium; Section of Infections of the Nervous System (B.S.); Viral Immunology Section (S.J.), National Institute of Neurological Disorders and Stroke (NINDS), National Institutes of Health (NIH), Bethesda, MD; Neurology Service (R.A.D.P., P.M.), Department of Clinical Neurosciences, Centre Hospitalier Universitaire Vaudois, University of Lausanne, Switzerland; Department of Neurology (V.V.P., P.M.), Cliniques Universitaires Saint-Luc, Université catholique de Louvain, Brussels, Belgium; Neuroimaging Research Unit (M.F.), Division of Neuroscience, IRCCS San Raffaele Scientific Institute, Milan, Italy; Translational Neuroradiology Section (D.S.R.), National Institute of Neurological Disorders and Stroke (NINDS), National In-stitutes of Health (NIH); and Department of Neurology (M.A.), Johns Hopkins University School of Medicine, Baltimore, MD.

Go to Neurology.org/NN for full disclosures. Funding information is provided at the end of the article.

The Article Processing Charge was funded by the authors.

Glossary

AUC = area under the curve; **CL** = cortical lesions; **DIR** = double inversion recovery; **DIS** = dissemination in space; **EDSS** = Expanded Disability Status Scale; **EPI** = echo planar imaging; **HTLV** = human T-lymphotropic virus; **ICC** = intraclass correlation coefficient; **MPRAGE** = magnetization prepared rapid gradient echo images; **MSSS** = Multiple Sclerosis Severity Scale; **NMOSD** = neuromyelitis optica spectrum disorder; **OCB** = oligoclonal bands; **OIND** = other inflammatory neurologic diseases; **PIRA** = progression independent of relapse and MRI activity; **ROC** = receiver operating characteristic; **SLE** = systemic lupus erythematosus.

Discussion

The combination of CVS, CL, and PRL can improve MS differential diagnosis. CL and PRL also correlated with clinical measures of poor prognosis, with PRL being a predictor of disability accrual independent of clinical/MRI activity.

Introduction

The diagnosis of multiple sclerosis (MS) can be challenging in clinical practice, as clinical and radiologic findings can sometimes be atypical for MS, and other diseases may mimic MS clinical and/or radiologic presentation.[1] MS diagnosis relies on demonstration of disease dissemination in space and time, following a clinical event characteristic of an MS exacerbation or documented clinical progression.[2] Over time, the McDonald MS diagnostic criteria have been iteratively modified and simplified, enabling earlier diagnosis and initiation of therapy.[3] However this approach has been criticized for decreasing the specificity of the diagnostic criteria and increasing the risk of MS misdiagnosis.[4,5]

To enhance diagnostic accuracy and reduce misdiagnosis,[4,5] researchers have been focusing on finding new and specific imaging biomarkers. Among them, the central vein sign (CVS), cortical lesion (CL), and paramagnetic rim lesion (PRL) have gained attention in the past 2 decades.[6] These markers can be visualized using specialized MRI techniques and have demonstrated high specificity for MS.[6-9] While the CVS reflects the perivenular development of inflammatory demyelination in white matter, PRLs indicate perilesional chronic inflammation and specifically the accumulation of iron-laden microglia/macrophages at the lesion edge after acute inflammation resolves.[10,11] CLs—focal abnormalities completely within the cortex or spanning both the cortex and the underlying white matter—are also a distinctive feature of MS.[12,13] Even if CLs have already been included in the last revision of McDonald criteria,[2] they are difficult to detect with conventional MRI protocols and are better identified with specialized MRI techniques.[12]

Although CVS, PRL, and CL are specific features of MS pathology, it is still unclear whether the combination of these 3 imaging biomarkers can further improve MS differential diagnosis and stratify patients with poor prognosis for therapeutic decision making. This research is crucial to ensure early and accurate diagnosis and improve patient outcomes.

In this study, we cross-sectionally evaluated the diagnostic performance of the CVS, CL, and PRL (taken alone and in combination) and prospectively analyzed their association with clinical outcomes, in a multicenter sample of MS and MS mimicking conditions drawn from 4 academic research hospitals in Europe and the United States.

Methods

Imaging, laboratory, and clinical data were prospectively collected under institutional review board–approved protocols in adults with clinical/MRI evidence of CNS involvement from 4 academic research hospitals: the NIH Clinical Center (Bethesda, MD), IRCCS San Raffaele Hospital (Milan, Italy), Saint Luc University Hospital (Brussels, Belgium), and Lausanne University Hospital (Lausanne, Switzerland).

Patient eligibility criteria included (1) age ≥18 years, (2) clinical/MRI evidence of CNS involvement and availability of a clinical diagnosis, and (3) availability of 3T 3-dimensional (3D) segmented T2*-weighted echo planar imaging (EPI) (for CVS and PRL assessment), and double inversion recovery (DIR) and/or T1-weighted magnetization prepared rapid gradient echo images (MPRAGE) (for CL assessment). Cases with diffuse leukoencephalopathy or with no discrete brain lesions were excluded from the analysis.

MRI Acquisition

In all centers, the 3T MRI protocol included a submillimeter isotropic 3D T2*-EPI sequence[14-16] for the detection of the CVS and PRL imaging biomarkers. CL assessment was performed on 3D-DIR and 3D-MPRAGE (Brussels) or 3D-synthetic-DIR (eFigure 1) generated from T1/T2 images[17] and 3D-MPRAGE (other centers).[12,18] Additional MRI methods are detailed in the eMethods and eTable 1 and 2.

Image Processing and Biomarker Assessment

Given that raters were partially involved in the recruitment of cases, all images were de-identified before analysis, as was the final diagnosis.

The CVS, CL, and PRL assessments were performed following previously published guidelines and methods (see eMethods for details).[12,19-21] For the CVS, the percentage of perivenular lesions across all eligible brain lesions[20] was determined in each participant, hereafter termed "proportion of CVS-positive lesions." Scans were further dichotomized as perivenular positive vs perivenular negative (CVS-positive/CVS-negative) based on the previously proposed "40% rule".[22,23] Considering that the proportion-based approach is time-consuming and not practical in daily clinical practice,[24] we also dichotomized patients as CVS-positive/CVS-negative based on the "Select3*"[24,25] and "Select6*" algorithms,[24,26] where a scan was considered as CVS-positive if there were respectively ≥3 or ≥6 eligible lesions that met the CVS-positive NAIMS criteria[20]; see the eMethods for details.

For the association with clinical measures, we dichotomized patients as having 0–4 and >4 PRL, based on a previously proposed clinically meaningful threshold of 4 PRL per patient,[27] and on the distribution of our cohort data. Brain volumes normalized to intracranial volume and total white matter T2-hyperintense lesion volume (hereafter, "T2 lesion load") were also computed; see the eMethods for details.

In each individual, CVS, CL, and PRL analysis was independently assessed by 2 trained investigators (P.M. and S.B. for Brussels and Lausanne cases; M.A. and M.S.M. for Milan and NIH cases), each unaware of the other's analysis and blinded to participant's diagnosis. All non-MS cases that were CVS-positive or bearing ≥1 PRL or ≥1 CL were jointly reviewed by M.A. and P.M. for final adjudication.

Clinical Outcome Assessment

To assess the prognostic value of the 3 biomarkers, MS cases were screened for progression independent of relapse and MRI activity (PIRA) over the 2 years after the study entry (corresponding to the research MRI scan). In case of clinical and/or MRI activity, the study entry baseline Expanded Disability Status Scale (EDSS) score was reset to a new baseline EDSS score obtained at least 3 months after the clinical/MRI relapse.[28] Patients with less than 18-month follow-up period free of clinical/MRI relapses were excluded from this analysis; see eMethods for details.

Statistical Analysis

The inter-rater reliability for CVS, CL, and PRL assessment was explored on a per-patient level using the one-way random model intraclass correlation coefficient (ICC).[29] A binomial logistic regression model, with CVS, CL, and PRL analyses as independent variables, was used to predict MS diagnosis (dependent variable). Receiver operating characteristic (ROC) curves were used to test the diagnostic performance of the CVS, CL, and PRL assessments, alone and in combination.

The relative importance to discriminate MS from non-MS of the CVS, of CL and PRL, as well as of the fulfillment of dissemination in space (DIS) criteria according to McDonald 2017[2] and Filippi et al. 2016,[30] and (when available) of the presence of CSF oligoclonal bands (OCB), was also explored by fitting a random forest model.

The association between CVS, CL, and PRL with MS disability (EDSS) and severity (Multiple Sclerosis Severity Scale [MSSS]) at the time of the research MRI scan (EDSS or MSSS as dependent variables) was assessed using linear regression models with PRL groups (PRL 0–4 and >4), number of CL or proportion of CVS-positive lesions as independent variables, alone and in combination, in addition to normalized brain volume and T2 lesion load as covariates. A binomial logistic regression model was used to predict the association of CVS, CL, PRL in addition to normalized brain volume, T2 lesion load, and patient's age and sex with PIRA at 2-year follow-up (PIRA as dependent variable). Additional statistical analysis methods are detailed in the eMethods.

Standard Protocol Approvals, Registrations, and Patient Consents

For this study, we received approval from the local ethical standards committee on human experimentation in each of the 4 academic research hospitals. Written informed consent was obtained from all patients participating in the study (consent for research).

Data Availability

The data that support the findings of this study are controlled by the respective centers and are not publicly available. Request to access the anonymized individual patient data should be forwarded to data controllers by the corresponding author. Written requests for access to the derived data will be considered by the corresponding author and a decision made about the appropriateness of the use of the data.

Results

From 2013 to May 2023, of the 297 consecutive eligible cases, we retrospectively included in this analysis 285 patients; 12 were excluded for motion-related MRI artifacts (Figure 1). Based on international published diagnostic criteria, included patients were grouped according to their clinical diagnosis. There were

- 185 individuals with MS, diagnosed according to the 2017 McDonald criteria[2] (113 relapsing-remitting, 47 secondary progressive, and 25 primary progressive)
- 38 individuals with other inflammatory neurologic diseases (OIND), including 12 cases of neuromyelitis optica spectrum disorder (NMOSD[31]; 11 were AQP4 antibody-positive and 1 seronegative) and 3 cases of myelin oligodendrocyte glycoprotein antibody-associated disease (MOGAD)[32]; 6 cases of systemic lupus erythematosus (SLE)[33]; 5 cases of Susac syndrome[34]; 6 cases of Behçet disease[35]; 3 cases of

Figure 1 CONSORT Flowchart

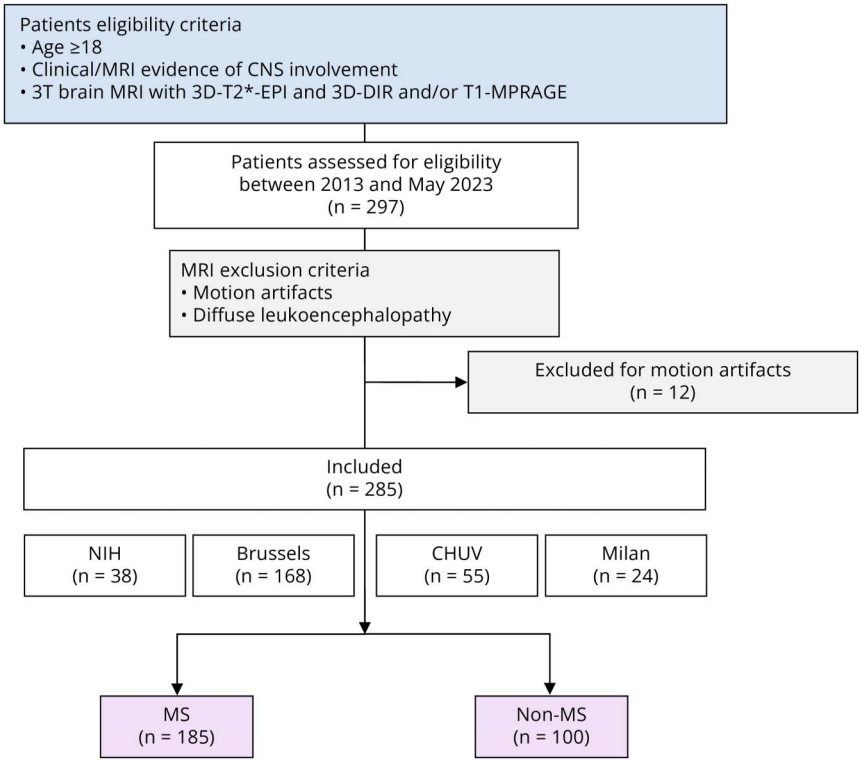

Flow chart summarizing patients' progress through the study. Brussels = Saint Luc University Hospital (Brussels, Belgium); CHUV = Lausanne University Hospital (Lausanne, Switzerland); EPI = echo planar imaging; Milan = San Raffaele University Hospital (Milan, Italy); MS = multiple sclerosis; NIH = National Institutes of Health, Clinical Center (Bethesda, MD).

Sjögren disease[36]; 2 cases of sarcoidosis[37]; and 1 case of ANCA-associated vasculitis.[38]

- 19 individuals infected by neurotropic viruses, randomly selected from larger data sets, including 9 individuals with human T-lymphotropic virus (HTLV)–associated myelopathy/tropical spastic paraparesis (HAM/TSP) and 10 with HIV infection, without other comorbidities, on antiretroviral therapy.
- 43 individuals affected by noninflammatory neurologic diseases (NIND), including small vessel disease and migraine. Demographic and clinical data are reported in Table 1.

Central Vein Sign

In the 285 scans analyzed, the CVS assessment ICC inter-rater agreement was 0.995 (95% confidence interval [CI] 0.980–0.999, $p < 0.001$). In agreement with previous data from the literature,[7,9] the proportion of CVS-positive lesions was remarkably high in our MS cohort (mean 78%, median 80%, range 23%–100%), compared with non-MS cases showing a very low proportion of CVS-positive lesions (mean 10%, median 0%, range 0%–50%; $p < 0.001$). Among non-MS cases, OIND and NIND showed the highest mean proportion of CVS-positive lesions (15% and 8%, respectively), followed by HAM/TSP (6%) and HIV (5%). When the 40% rule was applied,[22,23] 97% of MS cases were CVS-positive compared with 5% of non-MS cases (8% of OIND, 5% of NIND, and 0% for both HAM/TSP and HIV; Table 1, Figure 2, A and D). In line with this previously reported "40% rule" cutoff,[22,23] the optimal CVS proportion-based threshold identified in our cohort was 41%, which was associated with 95% specificity, 97% sensitivity, and an area under the ROC curve (AUC) of 0.993 (95% CI 0.988–0.999; Figure 3A). When the analysis was restricted to cases with at least 3 lesions suitable for CVS assessment (n = 258 of 285 cases), the diagnostic performance of CVS was comparable with the performance in the entire cohort (96% specificity, 97% sensibility and AUC of 0.994, 95% CI 0.989–0.999; $p = 0.71$).

When the Select3* simplified algorithm was applied,[24,25] 81% of MS cases were CVS-positive compared with 6% of non-MS cases (11% of HAM/TSP, 10% of OIND, 2% of NIND, and 0% of HIV; Table 1), with 93% specificity, 97% sensitivity, and AUC of 0.949 (95% CI 0.914–0.984; Figure 3A). When the Select6* simplified algorithm was applied,[24,26] 89% of MS cases were CVS-positive compared with 4% of non-MS cases (11% of HAM/TSP, 8% of OIND, 0% of NIND and HIV; Table 1), with a slight apparent decrease in diagnostic performance (95% specificity, 89% sensitivity, and AUC of 0.922, 95% CI 0.889–0.955; $p = 0.045$ Figure 3A).

Cortical Lesions

The CL assessment ICC inter-rater agreement was 0.998 (95% CI 0.995–0.999, $p < 0.001$). CLs were detected in 84%

Table 1 Cohort Characteristics

Characteristic	OIND	NIND	Neurotropic viruses		MS	Statistical analysis
			HTLV-infected HAM/TSP	HIV-infected		
Participants, n	38	43	9	10	185	—
Women, n (%)	27 (71)	33 (77)	6 (67)	1 (10)	115 (62)	X^2 $p = 0.002$
Age, mean (range), y	42 (21–77)	49 (26–75)	55 (37–75)	56 (45–62)	45 (20–76)	ANOVA $p = 0.001$
OCB positive of cases with CSF available for review, n (%)	11/26 (42)	0/7 (0)	9/9 (100)	—	130/147 (88)	X^2 $p < 0.001$
Fulfillment of dissemination in space MRI criteria according to McDonald revised MS criteria 2017[2]						
Cases, n (%)	24 (63)	6 (14)	1 (11)	0 (0)	185 (100)	X^2 $p < 0.001$
Fulfillment of dissemination in space MRI criteria according to Filippi et al. 2016[30]						
Cases, n (%)	16 (42)	4 (9)	0 (0)	0 (0)	167 (90)	X^2 $p < 0.001$
Perivenular lesion detection						
Proportion of CVS-positive lesions, mean (range)	15 (0–50)	8 (0–50)	6 (0–24)	5 (0–33)	78 (23–100)	ANOVA $p < 0.001$
Cases with ≥40% CVS-positive lesions,[a] n (%)	3 (8)	3 (7)	0 (0)	0 (0)	179 (97)	X^2 $p < 0.001$
Cases with positive Select3*,[a] n (%)	4 (10)	1 (2)	1 (11)	0 (0)	150 (81)	X^2 $p < 0.001$
Cases with positive Select6*,[a] n (%)	3 (8)	0 (0)	1 (11)	0 (0)	138 (89)	X^2 $p < 0.001$
Cortical lesion detection						
Cases with ≥1 CL, n (%)	6 (16)	1 (2)	2 (22)	0 (0)	156 (84)	ANOVA $p < 0.001$
Paramagnetic rim lesion detection						
Cases with ≥1 PRL, n (%)	6 (16)	1 (2)	0 (0)	0 (0)	111 (60)	ANOVA $p = 0.007$

Abbreviations: CL = cortical lesion; CVS = central vein sign; HAM/TSP = HTLV-associated myelopathy/tropical spastic paraparesis; HTLV = human T-lymphotropic virus; MS = multiple sclerosis; NIND = noninflammatory neurologic diseases; OCB = oligoclonal bands; OIND = other inflammatory/infectious neurologic diseases; PRL = paramagnetic rim lesion.
[a] Cases were dichotomized as overall CVS-positive vs CVS-negative based on the previously described "40% rule",[9,22,23] "Select3*,"[24,25] and "Select6*"[24,26] algorithms.

of MS cases (80% of RRMS, 91% of SPMS and 88% of PPMS) vs 9% of non-MS cases. HAM/TSP and OIND showed the highest detection rate of CL (2/9 [22%] and 6/38 [16%], respectively), followed by NIND (1/43 [2%]). No CL were detected in HIV cases (Table 1, Figure 2, B and E). The number of CL was higher in the MS cohort (total number 1518, mean 8, median 4, range 0–101), compared with non-MS cases (total number 20, mean 0, median 0, range 0–7; $p < 0.001$). The identification of ≥1 CL (optimal cutoff) was associated with 90% specificity, 84% sensitivity, and AUC of 0.897 (95% CI 0.865–0.931; Figure 3A). Among the 20 CL detected in non-MS cases, all (100%) were classified as leukocortical, and 4 of them (20%; all in the same case of SLE, Figure 4B) showed enhancement after contrast injection. In MS cases, most CL (1,464/1,518, 96%) were leukocortical and only a minority was purely intracortical.

Paramagnetic Rim Lesions

The PRL assessment ICC inter-rater agreement was 0.986 (95% CI 0.950–0.996, $p < 0.001$). PRL were detected in 60% of MS cases vs 7% of non-MS cases. Among non-MS cases, OIND showed the highest detection rate of PRL (6/38 [16%]), followed by NIND (1/43 [2%]). No PRL were detected in HIV and HAM/TSP cases (Table 1, Figure 2, C and F). The number of PRL was higher in the MS cohort (total number 604, mean 3, median 1, range 0–82), compared with non-MS cases (total number 13, mean 0, median 0, range 0–3, $p < 0.001$). The identification of ≥1 PRL (optimal cutoff) was associated with 93% specificity, 60% sensitivity, and AUC of 0.771 (95% CI 0.718–0.825; Figure 3A). Among the 13 PRL detected in non-MS cases, 4 (31%) were also CVS-positive; these lesions belonged to 3 patients respectively diagnosed with NMOSD-AQP4 positive, sarcoidosis (Figure 4A), and small vessel disease.

Figure 2 Central Vein Sign, Cortical Lesions, and Paramagnetic Rim Lesions in MS vs Non-MS

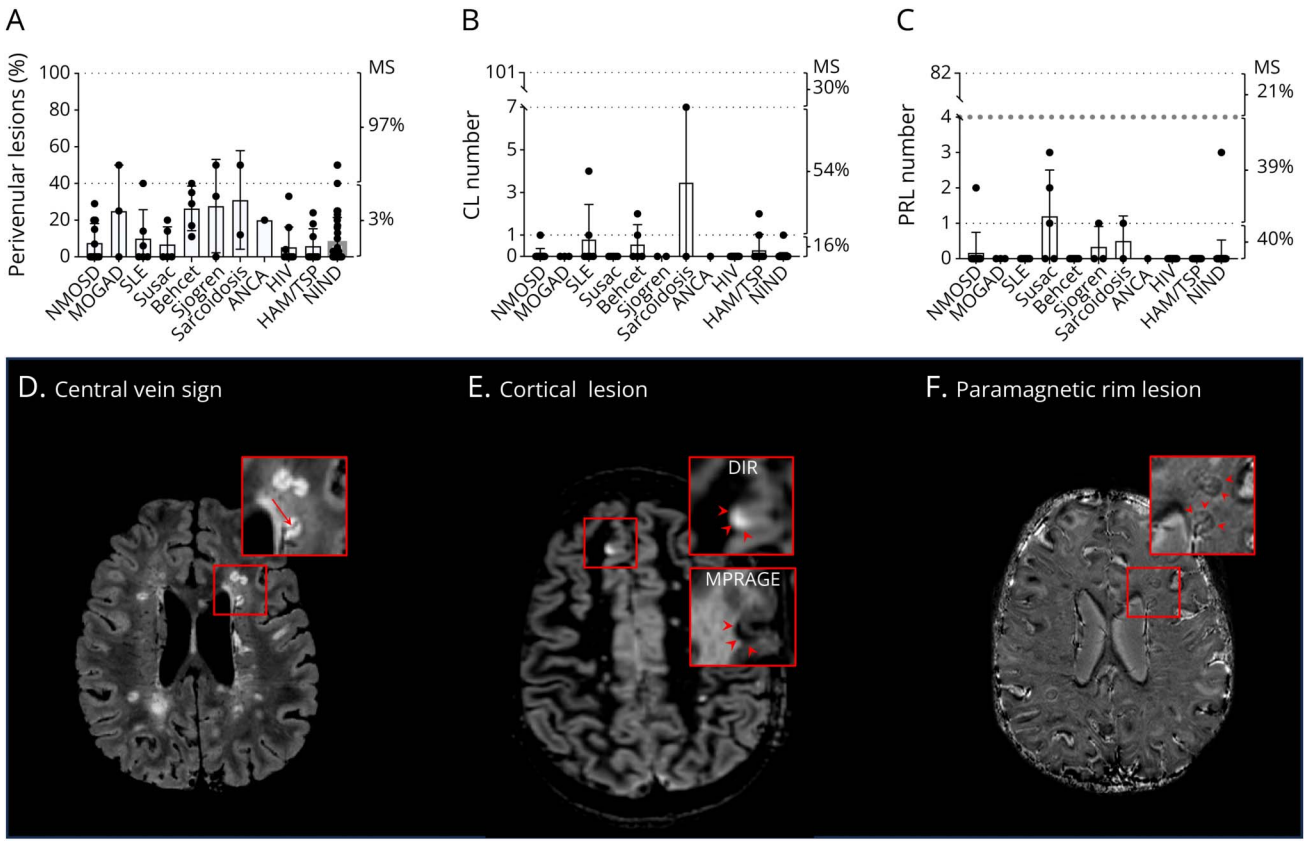

(A) Frequency of central vein sign–positive lesions, (B) number of cortical lesions and (C) of paramagnetic rim lesions in the 100 non-MS cases enrolled in the study (left vertical axis). Among the 185 enrolled MS cases (dotted lines, right vertical axis), most had ≥40% perivenular lesions (97%), ≥1 CL (84%) and ≥1 PRL (60%). Representative axial (D) FLAIR*, (E) DIR and MPRAGE, and (F) EPI-phase images showing, respectively, the CVS (arrow), CL (arrowhead) and PRL (arrowhead) biomarkers in an adult patient with RRMS. ANCA = ANCA-associated vasculitis; Behcet = Behçet disease; DIR = double inversion recovery images; HAM/TSP = human T-lymphotropic virus (HTLV)–associated myelopathy/tropical spastic paraparesis; HIV = HIV infection; MOGAD = myelin oligodendrocyte glycoprotein antibody–associated disease; MPRAGE = magnetization prepared rapid gradient echo images; NIND = noninflammatory neurologic diseases; NMOSD = neuromyelitis optica spectrum disorder; Sjogren = Sjögren disease; SLE = systemic lupus erythematosus; Susac = Susac syndrome.

CVS, CL, and PRL vs Established MS Diagnostic Criteria

The proportion of CVS-positive lesions alone showed a higher diagnostic performance when compared with the presence of CSF-specific OCB (52% specificity, 88% sensitivity, AUC 0.704, 95% CI 0.623–0.784; $p < 0.001$), the fulfillment of the McDonald 2017 DIS (65% specificity, 100% sensitivity, AUC 0.827, 95% CI 0.779–0.874; $p < 0.001$), and Filippi 2016 DIS criteria (80% specificity, 91% sensitivity, AUC 0.852, 95% CI 0.807–0.897; $p < 0.001$). The number of CL alone also showed a higher diagnostic performance compared with OCB ($p < 0.001$) and with McDonald 2017 DIS criteria ($p = 0.011$), but a similar performance when compared with Filippi 2016 DIS criteria ($p = 0.085$). The number of PRL alone showed a similar diagnostic performance compared with CSF specific OCB ($p = 0.203$) and McDonald 2017 DIS criteria ($p = 0.081$) and an inferior performance to Filippi 2016 DIS criteria ($p = 0.005$).

Combination of CVS, CL, and PRL

Among the 3 biomarkers, the proportion of CVS-positive lesions showed the highest diagnostic performance, followed by CL and PRL (Figure 3A; $p < 0.001$). When applying the simplified CVS algorithms, Select3* diagnostic performance was still superior to CL and PRL assessments (Figure 3A; $p = 0.019$ and $p < 0.001$, respectively), while Select6* showed a similar diagnostic performance to CL (Figure 3A; $p = 0.27$) but superior to PRL (Figure 3A; $p < 0.001$).

Using a weighted combined biomarker model (based on the logistic binomial regression, eTable 3), we estimated the probability of having MS based on the combination of the CVS, CL, and PRL assessments. The diagnostic performance of this model reached a higher diagnostic performance compared with 3 biomarkers alone, especially when the simplified Select 3* and Select 6* algorithms were used (Figure 3B; Table 2).

When the analysis was restricted to MS cases with less than 2 years of disease duration (n = 41) vs all non-MS cases (n = 100), the combination of CVS, CL, and PRL (weighted combined biomarker model) showed a higher diagnostic performance compared with the CVS alone, when the simplified Select3* algorithm was applied (Table 2).

Figure 3 Diagnostic Performance of the Central Vein Sign, Cortical Lesions, and Paramagnetic Rim Lesions

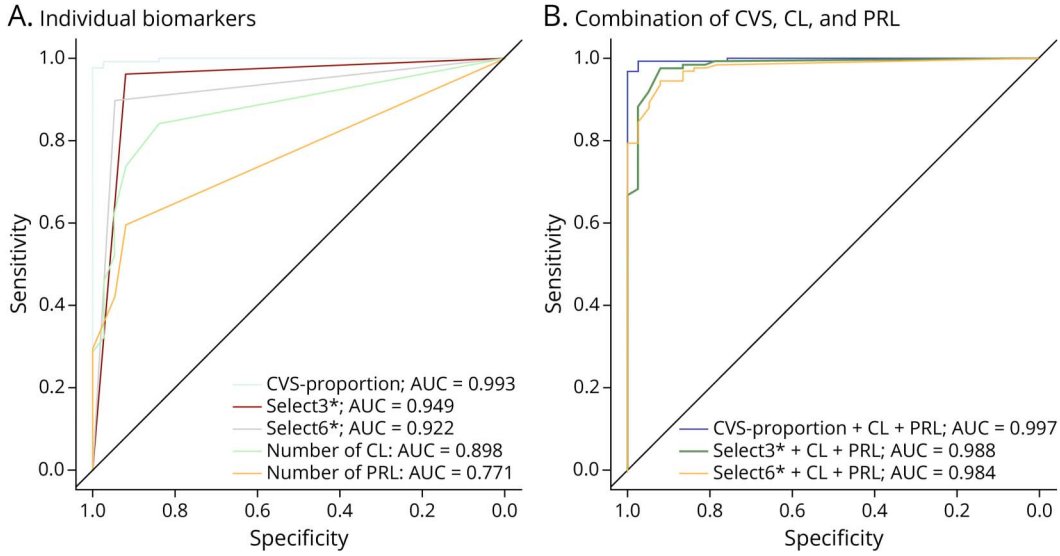

(A) ROC curves showing the performance of the central vein sign (as proportion of CVS-positive lesions, Select3*, and Select 6*), cortical lesions, and paramagnetic rim lesions in discriminating MS from non-MS cases. (B) ROC curves showing the performance of the weighted combined biomarker model (logistic binomial regression) in differentiating MS vs non-MS cases based on the combination of the specific proportion of CVS-positive lesions (or CVS-positivity/negativity based on the simplified Select3* or Select 6* algorithms) with the exact number of CL and PRL. AUC = area under the curve; CL = cortical lesions; CVS = central vein sign; PRL = paramagnetic rim lesions.

Figure 4 Central Vein Sign, Cortical Lesions, and Paramagnetic Rim Lesions in Non-MS Conditions

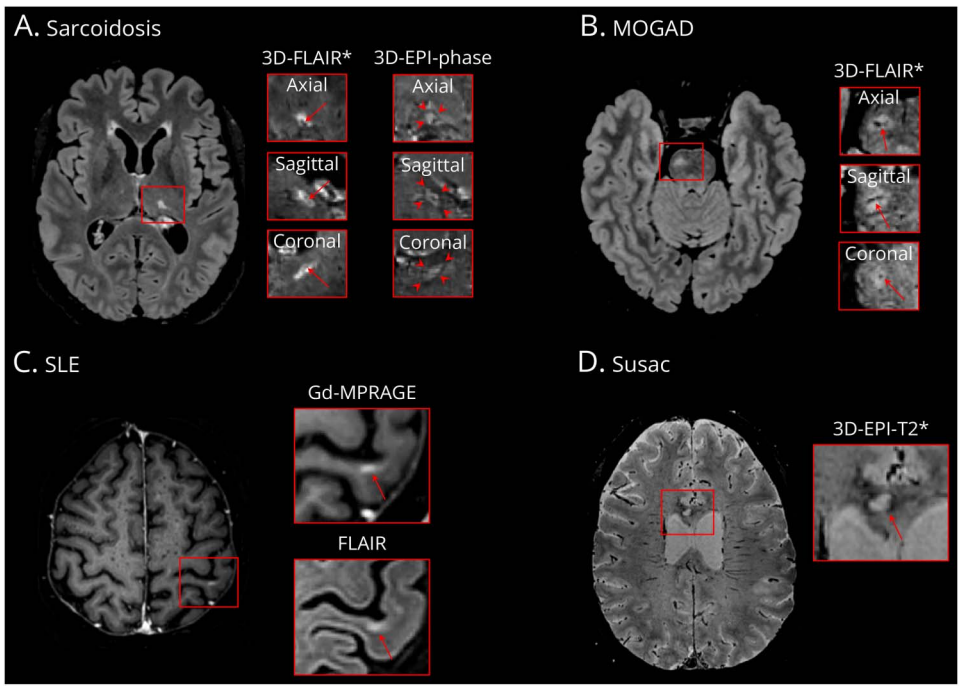

(A) Axial 3D-FLAIR, 3D-FLAIR*, and 3D-EPI-phase images of an adult patient with sarcoidosis. MS-like lesions bearing a central vein (arrows) and a paramagnetic rim (arrowhead) can occasionally be found also in non-MS conditions. Of note, this patient did not have any visible cortical lesions. (B) Axial 3D-FLAIR and 3D-FLAIR* images of an adult patient with MOGAD. Although MS-like lesions bearing a central vein (arrows) can occasionally be found also in non-MS conditions. However, this patient did not have any visible cortical or paramagnetic rim lesions. (C) Axial FLAIR and Gd-MPRAGE of an adult patient with systemic lupus erythematosus, showing a contrast enhancing cortical lesion (arrows). In this patient, the majority of lesions did not bear a central vein and none of them showed a paramagnetic rim. (D) Axial 3D-EPI-T2* magnitude images of an adult patient with Susac syndrome, showing one corpus callosum lesion bearing a paramagnetic rim on susceptibility-based images. Of note, this patient did not have any cortical nor central vein sign–positive lesions. EPI = segmented T2*-weighted echo planar imaging; Gd-MPRAGE = magnetization prepared rapid gradient echo MRI acquired post-IV injection of a paramagnetic gadolinium-based contrast agent; MOGAD = myelin oligodendrocyte glycoprotein antibody–associated disease; SLE = systemic lupus erythematosus.

Table 2 Differential Diagnosis Performance of CVS, CL, and PRL

Biomarker	Specificity	Sensitivity	AUC	vs CVS-proportion	vs Select 3*	vs Select 6*	vs CL	vs PRL
CVS								
CVS proportion	95%	97%	0.993	—	$p = 0.003$	$p < 0.001$	$p < 0.001$	$p < 0.001$
Select 3*	93%	97%	0.949	$p = 0.003$	—	$p = 0.047$	$p = 0.022$	$p < 0.001$
Select 6*	95%	89%	0.922	$p < 0.001$	$p = 0.047$	—	$p = 0.29$	$p < 0.001$
CL	91%	84%	0.898	$p < 0.001$	$p = 0.022$	$p = 0.29$	—	$p < 0.001$
PRL	93%	60%	0.771	$p < 0.001$	$p < 0.001$	$p < 0.001$	$p < 0.001$	—
CVS proportion + CL + PRL	99%	97%	0.997	$p = 0.047$	—	—	$p < 0.001$	$p < 0.001$
Select 3* + CL + PRL	93%	98%	0.988	—	$p = 0.002$	—	$p < 0.001$	$p < 0.001$
Select 6* + CL + PRL	94%	96%	0.984	—	—	$p < 0.001$	$p < 0.001$	$p < 0.001$
MS cases with less than 2 y of disease duration (n = 41) vs all non-MS cases (n = 100)								
CVS								
CVS proportion	95%	100%	0.997	—	$p = 0.024$	$p = 0.071$	$p = 0.001$	$p < 0.001$
Select 3*	93%	97%	0.901	$p = 0.024$	—	$p = 0.155$	$p = 0.054$	$p = 0.008$
Select 6*	95%	97%	0.962	$p = 0.071$	$p = 0.155$	—	$p = 0.026$	$p = 0.003$
CL	91%	80%	0.875	$p = 0.001$	$p = 0.054$	$p = 0.026$	—	$p = 0.53$
PRL	93%	72%	0.836	$p < 0.001$	$p = 0.008$	$p = 0.003$	$p = 0.53$	—
CVS proportion + CL + PRL	100%	100%	1.000	$p = 0.146$	—	—	$p = 0.001$	$p < 0.001$
Select 3* + CL + PRL	98%	94%	0.993	—	$p = 0.021$	—	$p = 0.001$	$p < 0.001$
Select 6* + CL + PRL	96%	97%	0.996	—	—	$p = 0.054$	$p = 0.001$	$p < 0.001$

Differential diagnosis performance of the 3 biomarkers, alone or in combination, compared with the one of the proportion of CVS-positive lesions (vs CVS-proportion), Select3* (vs Select3*), Select6* (vs Select3*), cortical lesions (vs CL), paramagnetic rim lesions (vs PRL).

When the analysis was restricted to patients with less than 3 lesions suitable for CVS assessment (n = 27, 9.5%), CL and PRL were found only in MS cases (CL: mean 2, median 1, range 0–12, $p < 0.001$; PRL: mean 2, median 1, range 0–6, $p = 0.02$) compared with non-MS cases. In this comparison, the diagnostic performance of CL (100% specific, 78% sensitivity, AUC 0.889, 95% CI 0.790–0.988) was comparable with that of PRL (100% specificity, 56% sensitivity, AUC 0.778, 95% CI 0.660–0.896; $p = 0.09$), and the identification of ≥1 CL or ≥1 PRL had 100% specificity, 83% sensitivity, and AUC of 0.917 (95% CI 0.828–0.999).

When the information on CVS (proportion of CVS-positive lesions, Select3*, and Select6*), CL, PRL, as well as fulfillment of McDonald 2017[2] and Filippi 2016 DIS criteria, and the presence of CSF specific OCB (CSF available for review = 189) were combined in a random forest model, the model achieved an AUC of 0.999 (95% CI 0.998–1.00). The variable importance analysis revealed that the most important predictors for MS classification were, in descending order of importance: proportion of CVS-positive lesions (MDG = 40), Select3* (MDG = 11), Select6* (MDG = 4), CL (MDG = 1), Filippi 2016 DIS criteria (MDG = 0.8), PRL (MDG = 0.3), CSF-specific OCB (MDG = 0.2), and McDonald 2017 DIS criteria (MDG = 0.1).

Association of CVS, CL, and PRL With MS Disability, MS Severity, and PIRA

In MS cases (n = 185), after adjusting for age and sex, both EDSS (β 0.05, 95% CI 0.03–0.07; $p < 0.001$) and MSSS (β 0.05, 95% CI 0.03–0.08; $p < 0.001$) were on average 0.05 points higher for every increase in CL number (EDSS and MSSS dependent variables). In a similar model, both EDSS (β 1.3, 95% CI 0.6–2.1; $p < 0.001$) and MSSS (β 2.0, 95% CI 1.0–2.9; $p < 0.001$) were on average 1.3 and 2.0 points higher in cases with >4 PRL cases compared with those with PRL 0–4. No association was found between the EDSS or the MSSS and the proportion of CVS-positive lesions (eTable 4). When CL and PRL were tested in the same model, the MSSS (dependent variable) was on average 1.7 points higher in cases with >4 PRL cases than in those with PRL 0–4 (β 1.7, 95% CI 0.6–2.7; $p = 0.002$). However, no other covariates, including the number of CL (β 0.02, 95% CI −0.01 to −0.06; $p = 0.2$), the normalized brain volume (β −3.8, 95% CI −8.0 to 0.3; $p =$

0.07), and the T2 lesion load (β 0.02, 95% CI −0.04 to 0.07; p = 0.5) were independently associated with MSSS. The results were similar when using the EDSS as the dependent variable, with PRL but not CL being associated with MS disability (eTable 5).

After a median follow-up period of 24 (range 18–35) months, 18 of 61 (29%) of MS cases experienced PIRA. Cases with >4 PRL were more likely to experience PIRA compared with those with PRL 0–4 (odds ratio [OR] 17.0, 95% CI 2.1–138.5; p = 0.008), whereas no other covariates, including number of CL (OR 1.0, 95% CI 0.9–1.0; p = 0.3), proportion of CVS-positive lesions (OR 1.0, 95% CI 0.9–1.0; p = 0.1), normalized brain volume (OR 0.8, 95% CI 0.6–1.2; p = 0.6), T2 lesion load (OR 1.0, 95% CI 0.9–1.0; p = 0.5), sex (OR 1.3, 95% CI 0.3–5.2; p = 0.7), and age (OR 1.0, 95% CI 0.9–1.1; p = 0.6) were associated with PIRA.

Discussion

In this cross-sectional multicenter academic study, we evaluated the diagnostic performance of the CVS, CL, and PRL, alone or in combination, to differentiate MS from a variety of non-MS neurologic conditions. We found that a high proportion of CVS-positive lesions, CL, and PRL was observed only rarely in neurologic conditions other than MS. Although the accuracy of the CVS in the differential diagnosis of MS was superior to that of CL and PRL taken alone, the combination of these 3 biomarkers achieved the best diagnostic performance. The contribution of CL and PRL was most evident when the more practical "Select3*"[24,25] and "Select6*"[24,26] algorithms were used to assess the CVS. Moreover, in cases where CVS could not be assessed (less than 3 lesions eligible for the CVS analysis),[20] CL and PRL achieved a good performance, alone or in combination, for differentiating MS from non-MS neurologic conditions. Besides their diagnostic value, CL and PRL also correlated with clinical measures of poor prognosis with PRL being an independent predictor of PIRA outcome at 2-year follow-up.

As expected,[7,9,39,40] a higher proportion of CVS-positive lesions was found in patients with MS compared with non-MS, resulting in high diagnostic sensitivity and specificity with an optimal CVS-positive lesion frequency cutoff of 41%, which is similar to the previously proposed "40% rule".[9,22,23] However, the exceptional CVS diagnostic performance and the specific CVS-positive lesion cutoff reported in our study is likely due to the adoption of the same optimized submillimetric 3D T2*-EPI sequence in all participating centers,[14,15] with minimal parameter adjustments and centralized postprocessing analysis. Recent findings suggest that the adoption of others imaging techniques (i.e., 2D SWI) for the CVS assessment is likely to result in a lower diagnostic performance.[39-41]

As in previous studies,[8,40,42] we found CL in the majority of MS cases and only rarely in non-MS cases. When compared with the proportion of CVS-positive lesions, the presence of a single CL provided high specificity but only moderate sensitivity for MS diagnosis. The CL detected in our MS sample were mostly of leukocortical type, consistent with previous reports that intracortical and subpial lesions are difficult to depict in vivo by 3T MRI.[43,44] Based on our non-MS sample, the few CL found in the other neurologic conditions were also of leukocortical type, making it difficult to distinguish CL of patients with MS vs CL in other non-MS conditions based only on their 3T MRI appearance. As already reported before, the number of CL in MS cases correlated with disability and severity scores,[45,46] supporting, beside their diagnostic utility, their association with a more aggressive disease phenotype.

The presence of PRL in MS indicates chronic, perilesional, unresolved inflammation,[10,47] an MRI feature that we rarely observed in MS-mimicking conditions. In agreement with previous observations,[7,48] we confirm here that this distinctive feature of MS lesions yields high specificity for MS diagnosis. Interestingly, we observed that about one-fourth of the PRL found in the non-MS cases were also CVS-positive, suggesting that MS-like lesions can rarely be observed also in non-MS conditions. Consistent with previous reports,[7,27] only slightly more than half of the MS cases harbored chronically inflamed lesions. Accordingly, although highly MS specific, PRL provided only low sensitivity for the diagnosis of MS. Aside from their diagnostic value, our data confirm that a higher PRL burden can identify MS cases with poorer prognosis,[7,10,27] since harboring >4 PRL is associated with higher disability and severity scores, including PIRA within the next 2 years. When coupled with recent findings on the natural history of these lesions (7T MRI phase changes during MS lesions evolution with fading rims over a median of 7 years),[47,49,50] these results further support the notion that PRL play an important role as drivers of future clinical progression.[21,51] Moreover, among the different MRI measures evaluated for their correlation with disease severity and PIRA, having >4 PRL was the strongest predictor; other measures, including CL, lost significance in the multivariable analysis. This finding suggests that PRL could serve as a more efficient prognostic biomarker compared with CL.

Comparing CVS, CL, and PRL, the proportion of CVS-positive lesions harbored the best diagnostic performance, with high sensitivity and specificity. CL and PRL were also highly specific but less sensitive for diagnosing MS. However, in routine clinical practice, the proportion-based approach for CVS analysis is not practical and time consuming,[24] especially in cases with high lesion burden. Therefore, simplified algorithms, such as "Select3*"[24,25] and "Select6*,"[24,26] have been proposed to preserve the CVS diagnostic performance and replace the need for complicated and time-consuming methods based on scoring of all white matter lesions. In our cohort, Select3* and Select6* showed an overall good diagnostic performance, slightly higher to that of CL for Select3*, and comparable for Select6*, and higher than that of PRL alone for both algorithms. These findings were further supported by the outcomes of the random forest model,

where the proportion of CVS-positive lesions, followed by the Select3* and Select6* rules, had the highest success in discriminating MS from non-MS cases.

The combination of CVS, CL, and PRL increased the diagnostic performance for MS compared to the 3 biomarkers alone, and this improvement was largest when the simplified Select3* and Select6* diagnostic algorithms were adopted for the CVS assessment. The weighted combined biomarker model presented here, based on a logistic binomial regression, offers the possibility to calculate the likelihood of having MS in individual patients. This calculation is based on the exact numbers of PRL and CL and on the specific frequency of CVS-positive lesions (or CVS positivity/negativity based on the simplified CVS algorithms), thus enabling a personalized diagnostic assessment.[52] What is the added value of combining these 3 MRI biomarkers for the diagnostic workup of MS? Our data suggest that the combination of the CVS, CL, and PRL biomarkers can help in the diagnostic workup of (1) non-MS cases harboring MRI features typical of MS (e.g., a high frequency of CVS and/or PRL-positive demyelinating lesions, and/or CL)[9,22]; (2) when one or more MRI biomarkers cannot be assessed or are atypical despite a suspected MS diagnosis (e.g., low frequency of CVS-positive lesions in older patients with small vessel disease comorbidities)[53]; and (3) patients with atypical clinical findings but with typical lesions on MRI (e.g.,; radiologically isolated syndrome or MS prodromal phase). Noteworthy, in nearly 10% of the scans analyzed, there were less than 3 lesions fulfilling the NAIMS eligibility criteria for CVS assessment.[20] In this context, the identification of at least one CL and/or one PRL may assist MS diagnosis even when CVS analysis cannot be performed.

This work has some limitations, including the cross-sectional design, the use of a convenience sample with a relatively low number of non-MS cases compared with MS cases and the absence of a confirmation cohort. Mitigating the final point is the consistency of our results with those of previous studies investigating one or 2 of the imaging biomarkers studied here. In addition, our cohort could not reflect the real-world diagnostic setting for newly presenting patients because the included patients with MS had a heterogeneous disease duration. Nonetheless, the performance of the weighted combined biomarker model was also tested in a small subgroup of patients with shorter disease duration. The overall CL detection rate in MS cases was slightly higher compared with previous studies.[8,42] This might be reconducted to the relatively high proportion of progressive MS phenotypes (where cortical pathology is known to be more prominent)[54,55] and to the adoption of multiple specialized MRI contrasts for CL detection. Similarly, the detection rate of PRL is likely to depends on the magnetic field strength, the susceptibility-based imaging acquisition, and the post-processing techniques applied,[56] thus PRL prevalence in MS may vary between different studies.[57-60] All those limitations should be considered when using the proposed diagnostic tool,[52] bearing in mind that it relies only on MRI data acquired with the specific imaging protocol of this study, and it has been trained only on the relatively small number of cases here included. Considering OCB, the relatively low differential diagnosis performance reported here[2] is likely to be related to the high frequency of inflammatory and infectious non-MS cases included, with all HTLV-infected patients showing positive CSF-specific OCB. Finally, because of stringent inclusion criteria such as a follow-up duration of at least 18 months and the absence of clinical and radiologic activity during the entire follow-up, PIRA analysis was only performed in a subset of 61 MS cases.

In conclusion, the presence of at least one CL and/or one PRL yields high specificity, and the "40%-CVS rule" both high specificity and sensitivity, for MS differential diagnosis. Despite the slight lower performance compared with proportion-based approach, the simplified Select3* and Select6* algorithms, more practical for use in clinical routine, yield overall good diagnostic performance. Specialized MRI protocols, combining CVS, CL, and PRL assessments can reliably improve MS differential diagnosis and should be considered for the next revision of MS diagnostic criteria, especially because, for CL and PRL, they also allow prognostic stratification of patients.

Acknowledgment

The authors thank the study participants; Avindra Nath (Section of Infections of the Nervous System, NIH/NINDS) and the neuroimmunology clinics in each center for recruiting and evaluating the patients and for coordinating the scans; Govind Nair and the NIH/NINDS Functional Magnetic Resonance Imaging Facility, Antonella Iadanza (IRCCS San Raffaele Hospital), Thierry Duprez, Sébastien de Laever (Cliniques universitaires Saint-Luc), Laurence Dricot (Université catholique de Louvain), and Julie Poujol (GE Healthcare) for assistance with 3T MRI scan acquisition and analysis.

Study Funding

S. Borrelli is supported by the Funds Claire Fauconnier, Ginette Kryksztein & José and Marie Philippart-Hoffelt, managed by the King Baudouin Foundation. A. Stölting has the financial support of the Fédération Wallonie Bruxelles - Fonds Spéciaux de Recherche (F.S.R). C. Vanden Bulcke has the financial support of the Fédération Wallonie Bruxelles - Fonds Spéciaux de Recherche (F.S.R). D.S. Reich is supported by the intramural Research Program of NIH/NINDS. M. Absinta is supported by research grants from the Conrad N. Hilton Foundation (Marylin Hilton Bridging Award for Physician-Scientists, grant 17313), the International Progressive MS alliance (21NS037), the Roche Foundation for Independent Research, the Cariplo Foundation (grant 1677), the FRRB Early Career Award (grant 1750327), and the National MS Society (NMSS RFA-2203-39325). P. Maggi research activity is supported by the Fondation Charcot Stichting Research Fund 2023, the Fund for Scientific Research (F.R.S, FNRS; grant 40008331), Cliniques universitaires Saint-Luc "Fonds de Recherche Clinique" and Biogen.

Disclosure

S. Borrelli received speaker/consulting honoraria from Sanofi, Roche, Janssen, Merck and Novartis, and research grants from Roche, Sanofi, and Brugmann Foundation not related to this work. M.S. Martire, A. Stölting, C. Vanden Bulcke, F. Guisset, C. Bugli, H. Yildiz, L. Pothen, V. Martinelli, B.R. Smith, S. Jacobson, R. Du Pasquier, report no disclosures relevant to the manuscript. S. Elands received consulting honoraria from Sanofi and Biogen. V. van Pesch received consulting honoraria from Biogen, Merck, Sanofi, BMS, Novartis, Janssen, Almirall, Roche, Alexion. M. Filippi is Editor-in-Chief of the Journal of Neurology, Associate Editor of Human Brain Map-ping, Neurologic Sciences, and Radiology; received compensation for consulting services from Alexion, Almirall, Biogen, Merck, Novartis, Roche, Sanofi; speaking activities from Bayer, Biogen, Celgene, Chiesi Italia SpA, Eli Lilly, Genzyme, Janssen, Merck-Serono, Neopharmed Gentili, Novar-tis, Novo Nordisk, Roche, Sanofi, Takeda, and TEVA; participation in Advisory Boards for Alexion, Biogen, Bristol-Myers Squibb, Merck, Novartis, Roche, Sanofi, Sanofi-Aventis, Sanofi-Genzyme, Takeda; scientific direction of educational events for Biogen, Merck, Roche, Celgene, Bristol-Myers Squibb, Lilly, Novartis, Sanofi-Genzyme; he receives research support from Biogen Idec, Merck-Serono, Novartis, Roche, Italian Ministry of Health, the Italian Ministry of University and Research, and Fondazione Italiana Sclerosi Multipla. D.S. Reich received research support from Abata and Sanofi. M. Absinta received consulting honoraria from Sanofi, GSK, Biogen and Abata Therapeutics. P. Maggi received consulting honoraria from Sanofi, Biogen and Merck. Go to Neurology.org/NN for full disclosures.

Publication History

Received by *Neurology: Neuroimmunology & Neuroinflammation* November 14, 2023. Accepted in final form March 13, 2024. Submitted and externally peer reviewed. The handling editor was Associate Editor Friedemann Paul, MD.

Appendix Authors

Name	Location	Contribution
Serena Borrelli, MD	Neuroinflammation Imaging Lab (NIL), Institute of NeuroScience, Université catholique de Louvain; Department of Neurology, Hôpital Erasme, Hôpital Universitaire de Bruxelles; Department of Neurology, Centre Hospitalier Universitaire Brugmann, Université Libre de Brussels, Belgium	Drafting/revision of the manuscript for content, including medical writing for content; major role in the acquisition of data; study concept or design; analysis or interpretation of data
Maria Sofia Martire, MD	Neurology Unit, IRCCS San Raffaele Hospital, Milan, Italy	Major role in the acquisition of data; analysis or interpretation of data
Anna Stölting, MSc	Neuroinflammation Imaging Lab (NIL), Institute of NeuroScience, Université catholique de Louvain, Brussels, Belgium	Major role in the acquisition of data; analysis or interpretation of data
Colin Vanden Bulcke, MSc	Neuroinflammation Imaging Lab (NIL), Institute of NeuroScience, Université catholique de Louvain, Brussels; ICTEAM Institute, Université catholique de Louvain, Louvain-la-Neuve, Belgium	Major role in the acquisition of data; analysis or interpretation of data
Edoardo Pedrini, PhD	Vita-Salute San Raffaele University; Translational Neuropathology Unit, Division of Neuroscience, IRCCS San Raffaele Scientific Institute, Milan, Italy	Major role in the acquisition of data; analysis or interpretation of data
François Guisset, MD	Neuroinflammation Imaging Lab (NIL), Institute of NeuroScience, Université catholique de Louvain, Brussels, Belgium	Major role in the acquisition of data; analysis or interpretation of data
Céline Bugli, PhD	Plateforme technologique de Support en Méthodologie et Calcul Statistique, Université catholique de Louvain, Brussels, Belgium	Analysis or interpretation of data
Halil Yildiz, MD	Department of Internal Medicine and Infectious Diseases, Cliniques Universitaires Saint-Luc, Université catholique de Louvain, Brussels, Belgium	Major role in the acquisition of data
Lucie Pothen, MD, PhD	Department of Internal Medicine and Infectious Diseases, Cliniques Universitaires Saint-Luc, Université catholique de Louvain, Brussels, Belgium	Major role in the acquisition of data
Sophie Elands, MD	Department of Neurology, Hôpital Erasme, Hôpital Universitaire de Bruxelles, Université libre de Bruxelles, Brussels, Belgium	Major role in the acquisition of data
Vittorio Martinelli, MD	Neurology Unit, IRCCS San Raffaele Hospital, Milan, Italy	Major role in the acquisition of data
Bryan Smith, MD	Section of Infections of the Nervous System, National Institute of Neurological Disorders and Stroke, National Insti-tutes of Health, Bethesda, MD	Major role in the acquisition of data
Steven Jacobson, PhD	Viral Immunology Section, National Institute of Neurological Disorders and Stroke (NINDS), National Institutes of Health (NIH), Bethesda, MD	Major role in the acquisition of data
Renaud A. Du Pasquier, MD	Neurology Service, Department of Clinical Neurosciences, Centre Hospitalier Universitaire Vaudois, University of Lausanne, Switzerland	Major role in the acquisition of data
Vincent Van Pesch, MD, PhD	Department of Neurology, Cliniques Universitaires Saint-Luc, Université catholique de Louvain, Brussels, Belgium	Major role in the acquisition of data

Continued

Appendix *(continued)*

Name	Location	Contribution
Massimo Filippi, MD	Neurology Unit, IRCCS San Raffaele Hospital; Vita-Salute San Raffaele University; Neuroimaging Research Unit, Division of Neuroscience, IRCCS San Raffaele Scientific Institute, Milan, Italy	Major role in the acquisition of data
Daniel S. Reich, MD, PhD	Translational Neuroradiology Section, National Institute of Neurological Disorders and Stroke (NINDS), National Institutes of Health (NIH), Bethesda, MD	Drafting/revision of the manuscript for content, including medical writing for content; major role in the acquisition of data
Martina Absinta, MD, PhD	Vita-Salute San Raffaele University; Translational Neuropathology Unit, Division of Neuroscience, IRCCS San Raffaele Scientific Institute, Milan, Italy; Department of Neurology, Johns Hopkins University School of Medicine, Baltimore, MD	Drafting/revision of the manuscript for content, including medical writing for content; major role in the acquisition of data; analysis or interpretation of data
Pietro Maggi, MD, PhD	Neuroinflammation Imaging Lab (NIL), Institute of NeuroScience, Université catholique de Louvain, Brussels, Belgium; Neurology Service, Department of Clinical Neurosciences, Centre Hospitalier Universitaire Vaudois, University of Lausanne, Switzerland; Department of Neurology, Cliniques Universitaires Saint-Luc, Université catholique de Louvain, Brussels, Belgium	Drafting/revision of the manuscript for content, including medical writing for content; major role in the acquisition of data; study concept or design; analysis or interpretation of data

References

1. Solomon AJ, Naismith RT, Cross AH. Misdiagnosis of multiple sclerosis: impact of the 2017 McDonald criteria on clinical practice. *Neurology*. 2019;92(1):26-33. doi:10.1212/WNL.0000000000006583
2. Thompson AJ, Banwell BL, Barkhof F, et al. Diagnosis of multiple sclerosis: 2017 revisions of the McDonald criteria. *Lancet Neurol.* 2018;17(2):162-173. doi:10.1016/S1474-4422(17)30470-2
3. Filippi M, Preziosa P, Arnold DL, et al. Present and future of the diagnostic work-up of multiple sclerosis: the imaging perspective. *J Neurol.* 2023;270(3):1286-1299. doi:10.1007/s00415-022-11488-y
4. Solomon AJ, Bourdette DN, Cross AH, et al. The contemporary spectrum of multiple sclerosis misdiagnosis: a multicenter study. *Neurology*. 2016;87(13):1393-1399. doi:10.1212/WNL.0000000000003152
5. Kaisey M, Solomon AJ, Luu M, Giesser BS, Sicotte NL. Incidence of multiple sclerosis misdiagnosis in referrals to two academic centers. *Mult Scler Relat Disord.* 2019;30:51-56. doi:10.1016/j.msard.2019.01.048
6. La Rosa F, Wynen M, Al-Louzi O, et al. Cortical lesions, central vein sign, and paramagnetic rim lesions in multiple sclerosis: emerging machine learning techniques and future avenues. *Neuroimage Clin.* 2022;36:103205. doi:10.1016/j.nicl.2022.103205
7. Maggi P, Sati P, Nair G, et al. Paramagnetic rim lesions are specific to multiple sclerosis: an international multicenter 3T MRI study. *Ann Neurol.* 2020;88(5):1034-1042. doi:10.1002/ana.25877
8. Cortese R, Prados Carrasco F, Tur C, et al. Differentiating multiple sclerosis from AQP4-neuromyelitis optica spectrum disorder and MOG-antibody disease with imaging. *Neurology*. 2023;100(3):e308–e323. doi:10.1212/WNL.0000000000201465
9. Maggi P, Absinta M, Grammatico M, et al. Central vein sign differentiates multiple sclerosis from central nervous system inflammatory vasculopathies: central Vein Sign. *Ann Neurol.* 2018;83(2):283-294. doi:10.1002/ana.25146
10. Absinta M, Sati P, Schindler M, et al. Persistent 7-tesla phase rim predicts poor outcome in new multiple sclerosis patient lesions. *J Clin Invest.* 2016;126(7):2597-2609. doi:10.1172/JCI86198
11. Absinta M, Sati P, Gaitán MI, et al. Seven-tesla phase imaging of acute multiple sclerosis lesions: a new window into the inflammatory process. *Ann Neurol.* 2013;74(5):669-678. doi:10.1002/ana.23959
12. Filippi M, Preziosa P, Banwell BL, et al. Assessment of lesions on magnetic resonance imaging in multiple sclerosis: practical guidelines. *Brain*. 2019;142(7):1858-1875. doi:10.1093/brain/awz144
13. Calabrese M, Filippi M, Gallo P. Cortical lesions in multiple sclerosis. *Nat Rev Neurol.* 2010;6(8):438-444. doi:10.1038/nrneurol.2010.93
14. Sati P, George IC, Shea CD, Gaitán MI, Reich DS. FLAIR*: a combined MR contrast technique for visualizing white matter lesions and parenchymal veins. *Radiology*. 2012;265(3):926-932. doi:10.1148/radiol.12120208
15. Sati P, Thomasson D, Li N, et al. Rapid, high-resolution, whole-brain, susceptibility-based MRI of multiple sclerosis. *Mult Scler.* 2014;20(11):1464-1470. doi:10.1177/1352458514525868
16. Absinta M, Sati P, Fechner A, Schindler MK, Nair G, Reich DS. Identification of chronic active multiple sclerosis lesions on 3T MRI. *AJNR Am J Neuroradiol.* 2018;39(7):1233-1238. doi:10.3174/ajnr.A5660
17. Manning AR, Beck ES, Schindler MK, et al. T_1/T_2 ratio from 3T MRI improves multiple sclerosis cortical lesion contrast. *J Neuroimaging*. 2023;33(3):434-445. doi:10.1111/jon.13088
18. Kober T, Granziera C, Ribes D, et al. MP2RAGE multiple sclerosis magnetic resonance imaging at 3T. *Invest Radiol.* 2012;47(6):346-352. doi:10.1097/RLI.0b013e31824600e9
19. Geurts JJG, Roosendaal SD, Calabrese M, et al. Consensus recommendations for MS cortical lesion scoring using double inversion recovery MRI. *Neurology*. 2011;76(5):418-424. doi:10.1212/WNL.0b013e31820a0cc4
20. Sati P, Oh J, Constable RT, et al. The central vein sign and its clinical evaluation for the diagnosis of multiple sclerosis: a consensus statement from the North American Imaging in Multiple Sclerosis Cooperative. *Nat Rev Neurol.* 2016;12(12):714-722. doi:10.1038/nrneurol.2016.166
21. Maggi P, Bulcke CV, Pedrini E, et al. B cell depletion therapy does not resolve chronic active multiple sclerosis lesions. *eBioMedicine*. 2023;94:104701. doi:10.1016/j.ebiom.2023.104701
22. Maggi P, Absinta M, Sati P, et al. The "central vein sign" in patients with diagnostic "red flags" for multiple sclerosis: a prospective multicenter 3T study. *Mult Scler.* 2020;26(4):421-432. doi:10.1177/1352458519876031
23. Tallantyre EC, Dixon JE, Donaldson I, et al. Ultra-high-field imaging distinguishes MS lesions from asymptomatic white matter lesions. *Neurology*. 2011;76(6):534-539. doi:10.1212/WNL.0b013e31820b7630
24. Ontaneda D, Sati P, Raza P, et al. Central vein sign: a diagnostic biomarker in multiple sclerosis (CAVS-MS) study protocol for a prospective multicenter trial. *Neuroimage Clin.* 2021;32:102834. doi:10.1016/j.nicl.2021.102834
25. Solomon AJ, Watts R, Ontaneda D, Absinta M, Sati P, Reich DS. Diagnostic performance of central vein sign for multiple sclerosis with a simplified three-lesion algorithm. *Mult Scler.* 2018;24(6):750-757. doi:10.1177/1352458517726383
26. Mistry N, Abdel-Fahim R, Samaraweera A, et al. Imaging central veins in brain lesions with 3-T T2*-weighted magnetic resonance imaging differentiates multiple sclerosis from microangiopathic brain lesions. *Mult Scler.* 2016;22(10):1289-1296. doi:10.1177/1352458515616700
27. Absinta M, Sati P, Masuzzo F, et al. Association of chronic active multiple sclerosis lesions with disability in vivo. *JAMA Neurol.* 2019;76(12):1474-1483. doi:10.1001/jamaneurol.2019.2399
28. Müller J, Cagol A, Lorscheider J, et al. Harmonizing definitions for progression independent of relapse activity in multiple sclerosis: a systematic review. *JAMA Neurol.* 2023;80(11):1232-1245. doi:10.1001/jamaneurol.2023.3331
29. Koo TK, Li MY. A guideline of selecting and reporting intraclass correlation coefficients for reliability research. *J Chiropractic Med.* 2016;15(2):155-163. doi:10.1016/j.jcm.2016.02.012
30. Filippi M, Rocca MA, Ciccarelli O, et al. MRI criteria for the diagnosis of multiple sclerosis: MAGNIMS consensus guidelines. *Lancet Neurol.* 2016;15(3):292-303. doi:10.1016/S1474-4422(15)00393-2
31. Wingerchuk DM, Banwell B, Bennett JL, et al. International consensus diagnostic criteria for neuromyelitis optica spectrum disorders. *Neurology*. 2015;85(2):177-189. doi:10.1212/WNL.0000000000001729
32. Banwell B, Bennett JL, Marignier R, et al. Diagnosis of myelin oligodendrocyte glycoprotein antibody-associated disease: international MOGAD Panel proposed criteria. *Lancet Neurol.* 2023;22(3):268-282. doi:10.1016/S1474-4422(22)00431-8
33. Petri M, Orbai AM, Alarcón GS, et al. Derivation and validation of the Systemic Lupus International Collaborating Clinics classification criteria for systemic lupus erythematosus. *Arthritis Rheum.* 2012;64(8):2677-2686. doi:10.1002/art.34473
34. Kleffner I, Dörr J, Ringelstein M, et al. Diagnostic criteria for Susac syndrome. *J Neurol Neurosurg Psychiatry*. 2016;87(12):1287-1295. doi:10.1136/jnnp-2016-314295
35. Criteria for diagnosis of Behçet's disease. International study group for Behçet's disease. *Lancet*. 1990;335(8697):1078-1080.
36. Shiboski CH, Shiboski SC, Seror R, et al. 2016 American College of Rheumatology/European League Against Rheumatism classification criteria for primary Sjögren's syndrome: a consensus and data-driven methodology involving three international patient cohorts. *Arthritis Rheumatol.* 2017;69(1):35-45. doi:10.1002/art.39859
37. Stern BJ, Royal W, Gelfand JM, et al. Definition and consensus diagnostic criteria for neurosarcoidosis: from the neurosarcoidosis consortium consensus group. *JAMA Neurol.* 2018;75(12):1546-1553. doi:10.1001/jamaneurol.2018.2295
38. Jennette JC, Falk RJ, Bacon PA, et al. 2012 revised international Chapel Hill consensus Conference Nomenclature of Vasculitides. *Arthritis Rheum.* 2013;65(1):1-11. doi:10.1002/art.37715

39. Castellaro M, Tamanti A, Pisani AI, Pizzini FB, Crescenzo F, Calabrese M. The use of the central vein sign in the diagnosis of multiple sclerosis: a systematic review and meta-analysis. *Diagnostics*. 2020;10(12):1025. doi:10.3390/diagnostics10121025
40. Cagol A, Cortese R, Barakovic M, et al. Diagnostic performance of cortical lesions and the central vein sign in multiple sclerosis. *JAMA Neurol*. 2024;81(2):143-153. doi:10.1001/jamaneurol.2023.4737
41. Sinnecker T, Clarke MA, Meier D, et al. Evaluation of the central vein sign as a diagnostic imaging biomarker in multiple sclerosis. *JAMA Neurol*. 2019;76(12):1446-1456. doi:10.1001/jamaneurol.2019.2478
42. Calabrese M, Battaglini M, Giorgio A, et al. Imaging distribution and frequency of cortical lesions in patients with multiple sclerosis. *Neurology*. 2010;75(14):1234-1240. doi:10.1212/WNL.0b013e3181f5d4da
43. Seewann A, Kooi EJ, Roosendaal SD, et al. Postmortem verification of MS cortical lesion detection with 3D DIR. *Neurology*. 2012;78(5):302-308. doi:10.1212/WNL.0b013e31824528a0
44. Kilsdonk ID, Jonkman LE, Klaver R, et al. Increased cortical grey matter lesion detection in multiple sclerosis with 7 T MRI: a post-mortem verification study. *Brain*. 2016;139(Pt 5):1472-1481. doi:10.1093/brain/aww037
45. Calabrese M, Poretto V, Favaretto A, et al. Cortical lesion load associates with progression of disability in multiple sclerosis. *Brain*. 2012;135(Pt 10):2952-2961. doi:10.1093/brain/aws246
46. Treaba CA, Granberg TE, Sormani MP, et al. Longitudinal characterization of cortical lesion development and evolution in multiple sclerosis with 7.0-T MRI. *Radiology*. 2019;291(3):740-749. doi:10.1148/radiol.2019181719
47. Dal-Bianco A, Grabner G, Kronnerwetter C, et al. Slow expansion of multiple sclerosis iron rim lesions: pathology and 7 T magnetic resonance imaging. *Acta Neuropathol*. 2017;133(1):25-42. doi:10.1007/s00401-016-1636-z
48. Clarke MA, Pareto D, Pessini-Ferreira L, et al. Value of 3T susceptibility-weighted imaging in the diagnosis of multiple sclerosis. *AJNR Am J Neuroradiol*. 2020;41(6):1001-1008. doi:10.3174/ajnr.A6547
49. Absinta M, Maric D, Gharagozloo M, et al. A lymphocyte–microglia–astrocyte axis in chronic active multiple sclerosis. *Nature*. 2021;597(7878):709-714. doi:10.1038/s41586-021-03892-7
50. Bozin I, Ge Y, Kuchling J, et al. Magnetic resonance phase alterations in multiple sclerosis patients with short and long disease duration. *PLoS ONE*. 2015;10(7):e0128386. doi:10.1371/journal.pone.0128386
51. Cagol A, Benkert P, Melie-Garcia L, et al. Association of spinal cord atrophy and brain paramagnetic rim lesions with progression independent of relapse activity in people with MS. *Neurology*. 2024;102(1):e207768. doi:10.1212/WNL.0000000000207768
52. Vanden Bulcke C, Wynen M, Detobel J, et al. BMAT: an open-source BIDS managing and analysis tool. *Neuroimage Clin*. 2022;36:103252. doi:10.1016/j.nicl.2022.103252
53. Guisset F, Lolli V, Bugli C, et al. The central vein sign in multiple sclerosis patients with vascular comorbidities. *Mult Scler*. 2021;27(7):1057-1065. doi:10.1177/1352458520943785
54. Calabrese M, Rocca MA, Atzori M, et al. Cortical lesions in primary progressive multiple sclerosis: a 2-year longitudinal MR study. *Neurology*. 2009;72(15):1330-1336. doi:10.1212/WNL.0b013e3181a0fee5
55. Reynolds R, Roncaroli F, Nicholas R, Radotra B, Gveric D, Howell O. The neuropathological basis of clinical progression in multiple sclerosis. *Acta Neuropathol*. 2011;122(2):155-170. doi:10.1007/s00401-011-0840-0
56. Bagnato F, Sati P, Hemond CC, et al. Imaging chronic active lesions in multiple sclerosis: a consensus statement. *Brain*. 2024:awae013. doi:10.1093/brain/awae013
57. Martire MS, Moiola L, Rocca MA, Filippi M, Absinta M. What is the potential of paramagnetic rim lesions as diagnostic indicators in multiple sclerosis? *Expert Rev Neurother*. 2022;22(10):829-837. doi:10.1080/14737175.2022.2143265
58. Sinnecker T, Schumacher S, Mueller K, et al. MRI phase changes in multiple sclerosis vs neuromyelitis optica lesions at 7T. *Neurol Neuroimmunol Neuroinflamm*. 2016;3(4):e259. doi:10.1212/NXI.0000000000000259
59. Wuerfel J, Sinnecker T, Ringelstein EB, et al. Lesion morphology at 7 Tesla MRI differentiates Susac syndrome from multiple sclerosis. *Mult Scler*. 2012;18(11):1592-1599. doi:10.1177/1352458512441270
60. Sinnecker T, Dörr J, Pfueller CF, et al. Distinct lesion morphology at 7-T MRI differentiates neuromyelitis optica from multiple sclerosis. *Neurology*. 2012;79(7):708-714. doi:10.1212/WNL.0b013e3182648bc8